

Ground-state phase diagram of the one-dimensional dimerized t - J model at quarter filling

S. Nishimoto

Graduate School of Science and Technology, Chiba University, Inage-ku, Chiba 263-8522, Japan

Y. Ohta

*Department of Physics, Chiba University, Inage-ku, Chiba 263-8522, Japan
and Graduate School of Science and Technology, Chiba University, Inage-ku, Chiba 263-8522, Japan*

(Received 11 May 1998)

The ground state of the one-dimensional dimerized t - J model at quarter filling is studied by a Lanczos exact-diagonalization technique on small clusters. We calculate the charge gap, spin gap, binding energy, Tomonaga-Luttinger-liquid parameter, Drude weight, anomalous flux quantization, etc. We thereby show that the two types of dimerization, i.e., a dimerization of hopping integral and a dimerization of exchange interaction play a mutually competing role in controlling the ground state of the system and this leads to the emergence of various phases including the Mott insulating, Tomonaga-Luttinger-liquid, and spin-gap-liquid phases. The ground-state phase diagram of the model is given on the parameter space of the dimerizations. [S0163-1829(99)02507-2]

I. INTRODUCTION

There are a number of low-dimensional correlated electron systems described by the Hubbard and t - J models at quarter-filling. One of the examples is the Bechgaard salts $(\text{TMTSF})_2X$ and $(\text{TMTTF})_2X$ with $X = \text{PF}_6$, ClO_4 , Br, etc., where there are three electrons in the two highest-occupied molecular-orbitals of a dimerized molecule, e.g., $(\text{TMTTF})_2$, and the system is at $\frac{3}{4}$ filling in terms of electrons, which corresponds to the quarter-filling in terms of holes.¹ In this system, dimerization of the molecules is known to play an essential role: depending primarily on the strength of dimerization, there appears a variety of electronic phases, such as antiferromagnetic insulating, paramagnetic metallic, and superconducting phases.¹ Some theoretical calculations of the dimerized Hubbard models have been done to clarify the nature of this system.^{2,3}

Another example is the transition-metal oxide NaV_2O_5 which is reported to be a quarter-filled ladder system, exhibiting a spin-Peierls-like phase transition accompanied by a charge ordering.^{4,5} This system may also be regarded as a dimerized system at quarter filling if we may assume that two V ions on each rung of the ladder form a dimer molecule.^{5,6} The CuO_3 chains of $\text{PrBa}_2\text{Cu}_3\text{O}_7$ are also referred to as a one-dimensional (1D) system around quarter filling.^{7,8} Effects of the lattice dimerization on the correlated electron systems in two dimensions have also been studied in connection with cuprate superconductivity, where the spin-gap phenomena above T_c have attracted much attention. The simplest possible model that exhibits a spin gap that can survive against hole doping may be a dimerized t - J model with an alternating exchange interaction, where an enhancement of the singlet superconducting correlation has been suggested.⁹

Motivated by such developments in the field, we study in this paper the 1D dimerized t - J model at quarter filling, of which not very much is known so far. The model we study is defined by the Hamiltonian,

$$H = -t_1 \sum_{\langle ij \rangle \sigma} (\hat{c}_{i\sigma}^\dagger \hat{c}_{j\sigma} + \text{H.c.}) - t_2 \sum_{\langle kl \rangle \sigma} (\hat{c}_{k\sigma}^\dagger \hat{c}_{l\sigma} + \text{H.c.}) + J_1 \sum_{\langle ij \rangle} \left(\mathbf{S}_i \cdot \mathbf{S}_j - \frac{n_i n_j}{4} \right) + J_2 \sum_{\langle kl \rangle} \left(\mathbf{S}_k \cdot \mathbf{S}_l - \frac{n_k n_l}{4} \right), \quad (1)$$

where $\hat{c}_{i\sigma}^\dagger = c_{i\sigma}^\dagger (1 - n_{i-\sigma})$ is the constrained electron-creation operator at site i and spin $\sigma (= \uparrow, \downarrow)$, \mathbf{S}_i is the spin- $\frac{1}{2}$ operator, and n_i is the electron-number operator; hereafter we refer to the fermionic particle as ‘‘electron,’’ which corresponds to, e.g., the hole in the organic compounds. We use the 1D lattice shown in Fig. 1; $\langle ij \rangle$ stands for nearest-neighbor bonds with parameters t_1 and J_1 and $\langle kl \rangle$ for those with parameters t_2 ($\geq t_1$) and J_2 ($\geq J_1$). The model tends to the usual homogeneous t - J model when there is no dimerization ($t_1 = t_2$ and $J_1 = J_2$), a concept that has been the focus of a considerable amount of research;¹⁰⁻¹³ whereas in the limit of strong dimerization, the model represents an assembly of isolated dimers. We retain the relations between parameters t and J obtained from perturbation, i.e., $J_1 = 4t_1^2/U$ and $J_2 = 4t_2^2/U$, in order to reduce the number of parameters, where U is the corresponding on-site Hubbard interaction. We thereby keep a relation $J_1/J_2 = (t_1/t_2)^2$. We thus have three independent parameters, and if we take t_2 as a unit of energy, we are left with two parameters, for which we will take parameters representing t and J dimerization (for which a specific definition is given below).

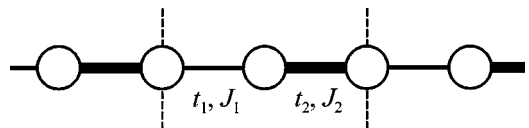


FIG. 1. Schematic representation of the 1D dimerized t - J model. The nearest-neighbor bonds have either t_1 and J_1 (thin solid line) or t_2 and J_2 (bold line). The unit cells, each of which contains two sites, are indicated by dashed lines.

We employ a Lanczos exact-diagonalization technique,¹⁴ which is used to obtain energies of the ground state and a few low-lying excited states. We denote the number of lattice sites by N_s and the numbers of up- and down-spin electrons by N_\uparrow and N_\downarrow , respectively. The electron density is then given by $n = (N_\uparrow + N_\downarrow)/N_s$, so that $n = 1$ represents the half-filled system. Here we restrict ourselves to the case of $n = 1/2$, i.e., quarter-filling. We use the finite-size systems of sizes 4, 6, and 8 unit cells (or 8, 12, and 16 sites, respectively). In order to achieve a systematic convergence to the thermodynamic limit, we choose periodic boundary condition for $N_\uparrow + N_\downarrow = 4m + 2$ and antiperiodic boundary condition for $N_\uparrow + N_\downarrow = 4m$ where m is an integer.

We will examine the ground-state properties by calculating the charge gap, spin gap, Luttinger liquid parameters, anomalous flux quantization, etc., as a function of the dimerization strength. We will thereby show that the competition between the two types of dimerization leads to various ground-state phases such as a Mott insulating phase, Tomonaga-Luttinger-liquid phase, spin-gap-liquid phase, etc. The ground-state phase diagram of the model is thereby given.

This paper is organized as follows: In Sec. II, we present the calculated charge and spin gaps and clarify the mechanism of the insulator-metal (or superconductor) transition. In Sec. III, we calculate the Tomonaga-Luttinger-liquid properties of the model and also discuss a possibility of singlet superconductivity. In Sec. IV we present a phase diagram of the system by summarizing the results given in Secs. III and IV. Conclusions are given in Sec. V.

II. INSULATOR-METAL TRANSITION

In this section, we calculate the charge gap, spin gap, and binding energy of the model, and discuss the mechanism of insulator-metal (or superconductor) transition of the system. First let us introduce two parameters for dimerization; i.e., the strength of dimerization in the hopping integral defined as

$$\tilde{t}_d = \frac{t_2 - t_1}{t_1}, \quad (2)$$

which we call t dimerization, and the strength of dimerization in the exchange interaction defined as

$$\tilde{J}_d = \frac{J_2 - J_1}{t_1}, \quad (3)$$

which we call J dimerization. We also take J_2/t_2 as a measure of the strength of J dimerization because if we keep \tilde{t}_d constant (>0) then $J_2/t_2 \propto \tilde{J}_d$. These are the key parameters that control the electronic state of the system; the t dimerization has the effect leading to the repulsive interaction among electrons that act when different spins come in a single dimer, and the J dimerization has the effect promoting the spin-singlet formation between spins coming in a single dimer. These effects manifest themselves in the electronic state of an isolated t - J dimer with an electron. The single-particle gap of the dimer is given as $U_{\text{dimer}} = 2t - J$, where t and J are the hopping and exchange parameters of the single bond, and thus U_{dimer} may be regarded as the effective

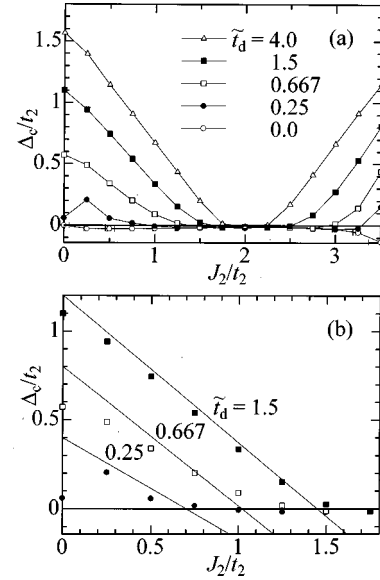


FIG. 2. (a) Charge gap Δ_c/t_2 as a function of J_2/t_2 . (b) Perturbation estimate of the charge gap compared with exact-diagonalization data.

Hubbard-like interaction of the dimer. The value of U_{dimer} can be either positive or negative depending on whether the value J/t is smaller or larger than 2. The competing effects of the two types of dimerization may thus be explained in the limit of strong dimerization. Now let us examine whether the competition between the effects of two types of dimerization in the 1D system can lead to the insulator-metal (or superconductor) transition. For this purpose we calculate the charge gap, spin gap, and binding energy.

A. Charge gap

The charge gap may be defined by

$$\Delta_c = \frac{1}{2} \{ [E_0(N_\uparrow + 1, N_\downarrow) - E_0(N_\uparrow, N_\downarrow)] - [E_0(N_\uparrow, N_\downarrow) - E_0(N_\uparrow - 1, N_\downarrow)] \}, \quad (4)$$

where $E_0(N_\uparrow, N_\downarrow)$ is the ground-state energy of the system with N_\uparrow up-spin and N_\downarrow down-spin electrons. This expression is evaluated for clusters of sizes of 8, 12, and 16 sites; throughout the paper we use a linear extrapolation of the calculated data for these clusters with respect to $1/N_s$ in order to estimate the value at the infinite system size. It is not quite sufficient as a finite-size analysis to use only three different system sizes, but because all the data presented behave fairly monotonically as the system size changes and also because the proposed physical picture is intuitively quite clear as explained above, we expect that the extrapolated results should correctly reflect the true thermodynamic limit at least qualitatively. Employing a more sophisticated scaling formula, using data for larger size systems, will be required to obtain more convincing results; however, this will be left for future work. The purpose of this paper is to examine and present the overall behavior of our model, of which even a rough feature is not known so far.

The calculated results for Δ_c as a function of the t and J dimerizations (i.e., \tilde{t}_d and J_2/t_2) are shown in Fig. 2(a), where we note some unphysical small negative values, which

are due to the errors of the finite-size scaling. Let us first see the case where there is no dimerization ($t_1=t_2$ and $J_1=J_2$), i.e., the homogeneous t - J model. A number of studies^{10–13} have shown that there is no charge gap $\Delta_c/t_2=0$ in the entire region of J_2/t_2 (except in the region of phase separation). Our result is consistent with this. In case where there is dimerization, the charge gap opens as seen in Fig. 2(a). At $J_2/t_2 \rightarrow 0$ the system is equivalent to the 1D dimerized Hubbard model at $U \rightarrow \infty$, so that the dimerization gap of the size $\Delta_D=2(t_2-t_1)$ opens at the Brillouin zone boundary, which is the charge gap. In other words, the separation between the lowest unoccupied (antibonding) band and the highest completely occupied (bonding) band is given by Δ_D . In the real-space picture, there is one electron per dimer, i.e., the number of electrons is equal to the number of dimers, and by regarding the dimer as a site one may have an effective half-filled band with the effective Coulomb repulsion of $U_{\text{eff}}=\Delta_D$. We thus have a Mott insulator due to t dimerization.

With increasing J dimerization J_2/t_2 , we find that Δ_c/t_2 decreases and becomes zero at a value $J_2/t_2=(J_2/t_2)_c^{\text{charge}}$ where the gap closes. $(J_2/t_2)_c^{\text{charge}}$ represents the critical strength of J dimerization at which a transition from insulating phase to metallic (or superconducting) phase occurs. This may be explained as follows: In the insulating phase ($\Delta_c/t_2 > 0$), the effective repulsion U_{eff} is given by the difference between loss of the kinetic energy and gain in the exchange interaction when one brings two electrons into a dimer, i.e., $U_{\text{eff}}=2(t_2-t_1)-J_2$. Thus, with increasing J_2/t_2 , the measure of the gap U_{eff} decreases, and at some value of J_2/t_2 the charge gap closes. In the small J -dimerization limit, we may use the perturbation theory with respect to J_2/t_2 (or J_1/t_1).³ After a straightforward calculation we obtain the result for the charge gap:

$$\Delta_c=2(t_2-t_1)\left[1-\frac{\ln 2}{\pi}\left(\frac{J_1}{t_1}+\frac{J_2}{t_2}\right)\ln\frac{4(t_1+t_2)}{t_2-t_1}\right]. \quad (5)$$

In the limit of $J_2 \rightarrow 0$ and $J_1 \rightarrow 0$, this expression reduces to $\Delta_c=2(t_2-t_1)$, which is equal to Δ_D defined above. We compare the exact-diagonalization data with this analytical expression in Fig. 2(b) where we find a good agreement.

With increasing J_2/t_2 further, we find that at some J_2/t_2 value the charge gap starts to increase again [see Fig. 2(a)], at which point the spin gap opens as we will see below. This is because Δ_c reflects the effect of the singlet binding energy in the charge-gapless region.

B. Spin gap and binding energy

The spin gap may be defined by

$$\Delta_s=E_0(N_\uparrow+1, N_\downarrow-1)-E_0(N_\uparrow, N_\downarrow). \quad (6)$$

The calculated results for Δ_s as a function of the t and J dimerizations are shown in Fig. 3. When there is no dimerization, the results obtained are consistent with a recent result for the t - J model.¹³ In a small J_2/t_2 limit we have $\Delta_s \rightarrow 0$ because there is no spin correlation in the system. With increasing J_2/t_2 with a fixed strength of t dimerization, we find that the spin gap opens at some J_2/t_2 value, which we define as $(J_2/t_2)_c^{\text{spin}}$, the critical strength of J dimerization at

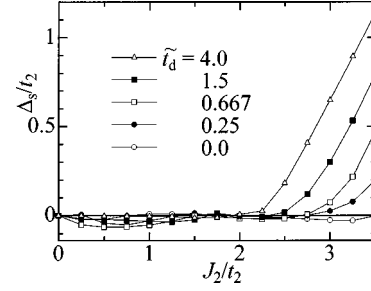


FIG. 3. Spin gap Δ_s/t_2 as a function of J_2/t_2 .

which the spin gap opens. We find that the spin gap remains finite in the region between $J_2/t_2=(J_2/t_2)_c^{\text{charge}}$ and the larger J_2/t_2 value at which the phase separation occurs. We also find that with increasing \tilde{t}_d , the critical strength $(J_2/t_2)_c^{\text{spin}}$ becomes smaller and at the same time Δ_s/t_2 increases. This means that the spin gap is enhanced by increasing the t dimerization.

We note that the relation $(J_2/t_2)_c^{\text{spin}} > (J_2/t_2)_c^{\text{charge}}$ always holds. This suggests that there exist two types of metallic regions in the model; one is the phase where there are both gapless spin and gapless charge modes, and the other is the phase where there is a gap only in the spin excitation, which are the so-called Tomonaga-Luttinger (TL) liquid region and spin-gap liquid region, respectively. We will discuss this further in Sec. III.

A simple picture may be given to the case of strong J dimerization where the spin-gap formation is ensured. When an even number of electrons exist, in the lowest-order perturbation of t_2/J_2 , two electrons with opposite spins always make a pair on the dimerized bond and gain the singlet formation energy $3J_2/4$. The electrons hop only as a pair tunneling through the virtual pair breaking in the fourth order of t_1/J_1 or t_2/J_2 . The effective Hamiltonian is then of the form

$$H_{\text{eff}}=-\tilde{t}(s_i^\dagger s_{i+2}+\text{H.c.}), \quad (7)$$

where

$$s_i^\dagger=\frac{1}{\sqrt{2}}(c_{i\uparrow}^\dagger c_{i+1\downarrow}^\dagger-c_{i\downarrow}^\dagger c_{i+1\uparrow}^\dagger) \quad (8)$$

is the singlet Bose operator at site i (even number) and

$$\tilde{t}=\left(2+\frac{t_1^2}{t_2^2-t_1^2}\right)\frac{t_1^2 t_2^2}{J_2^3} \quad (9)$$

is the effective hopping parameter of the boson. The Hamiltonian Eq. (7) may be derived in the same way as the effective Hamiltonian of the attractive Hubbard model in the strong-coupling limit.^{9,15}

We also calculate the binding energy defined as

$$\Delta_B=[E_0(N_\uparrow+1, N_\downarrow-1)-E_0(N_\uparrow, N_\downarrow)]-2[E_0(N_\uparrow+1, N_\downarrow)-E_0(N_\uparrow, N_\downarrow)], \quad (10)$$

which is negative if two electrons minimize their energy by producing a bound state, and indicates a possible superconductivity. This value is meaningless unless the system is me-

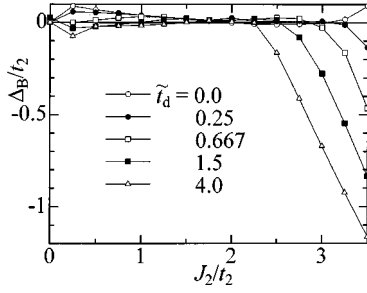


FIG. 4. Binding energy Δ_B/t_2 as a function of J_2/t_2 .

talic or $J_2/t_2 > (J_2/t_2)_c^{\text{charge}}$. In Fig. 4, we show calculated results for Δ_B as a function of J_2/t_2 , where we find $\Delta_B \approx 0$ for all values of $\tilde{t}_d > 0$ until $J_2/t_2 = (J_2/t_2)_c^{\text{spin}}$ is reached, and at this critical point Δ_B starts to decrease suddenly. This means that a bound state of two holes is formed in the entire region of the spin-gap phase and the binding energy is enhanced as J_2/t_2 is increased. We also note that at constant J_2/t_2 the value of Δ_B increases with increasing of \tilde{t}_d ; i.e., the singlet binding energy is enhanced by the t dimerization.

III. LUTTINGER-LIQUID BEHAVIOR

It is well known that the 1D interacting fermion systems may be related to the Fermi-gas model in the continuum limit, where there are two different regimes, the Tomonaga-Luttinger (TL) regime and Luther-Emery (LE) regime. As for liquid phases, the essential difference between the two lies in the spin degrees of freedom; the TL liquid region is characterized by the liquid phase with both a gapless spin mode and a gapless charge mode, whereas in the LE-liquid region the charge degrees of freedom is described by the TL liquid but the spin degrees of freedom have a gap (which we call the spin-gap liquid region here). According to the TL liquid theory,^{16–18} various combinations of the parameters K_ρ and K_σ describe the critical exponents of correlation functions of the system. In the absence of magnetic field, the dimerized t - J model is isotropic in spin space, so that $K_\sigma = 1$ holds, and we are left with the only parameter K_ρ .

In the TL region, the spin and charge correlation functions show a power-law dependence as

$$\langle S_i^z S_{i+r}^z \rangle \sim e^{2ik_F r / r^{K_\rho + K_\sigma}} \quad (11)$$

and

$$\langle n_i n_{i+r} \rangle \sim e^{2ik_F r / r^{K_\rho + K_\sigma} + e^{4ik_F r / r^{4K_\rho}}, \quad (12)$$

respectively. We see that, for $K_\rho < 1$, $2k_F$ -SDW or $2k_F$ -CDW (where SDW is spin-density wave and CDW is charge-density wave) are enhanced and diverged, whereas for $K_\rho > 1$, pairing fluctuations dominate. In the spin-gap liquid region, on the other hand, the spin gap opens and the $2k_F$ -SDW correlation decays exponentially. Because the contribution from spin excitations vanishes, the critical exponent of $2k_F$ -CDW also changes and the asymptotic form is given by

$$\langle n_i n_{i+r} \rangle \sim e^{2ik_F r / r^{K_\rho}}. \quad (13)$$

Thus, in the region with $K_\rho > 1$, the singlet spin correlation dominates over the $2k_F$ -CDW correlation.

The relations between the correlation exponent K_ρ and the low-energy behavior of the model given below are useful for the evaluation of K_ρ ; first, the parameter K_ρ is obtained from the charge compressibility κ and charge velocity v_c as

$$K_\rho = \frac{\pi}{2} v_c \kappa. \quad (14)$$

The charge velocity may be determined by

$$v_c = \frac{N_s}{2\pi} (E_{1,s=0} - E_0), \quad (15)$$

where $E_{1,s=0}$ is the energy of the lowest charge mode (measured from the ground-state energy E_0) at a neighboring k point. The inverse compressibility is given by

$$\begin{aligned} \frac{1}{n^2 \kappa} &= \frac{1}{N_s} \frac{\partial^2 E_0}{\partial n^2} \\ &= \frac{2}{N_s} \{ [E_0(N_\uparrow + 1, N_\downarrow + 1) - E_0(N_\uparrow, N_\downarrow)] \\ &\quad - [E_0(N_\uparrow, N_\downarrow) - E_0(N_\uparrow - 1, N_\downarrow - 1)] \}^{-1}. \end{aligned} \quad (16)$$

The parameter K_ρ is also related to the Drude weight D , the weight of the zero-frequency peak in the optical conductivity σ_ω , and may be obtained by considering the curvature of the ground-state energy level as a function of the threaded flux:^{19–22}

$$D = 2v_c K_\rho = \frac{N_s}{4\pi} \frac{\partial^2 (E_0)}{\partial \Phi^2}. \quad (17)$$

Equations (14)–(17) provide us with independent conditions on K_ρ , v_c , and D , which can be used to evaluate the TL-liquid parameter and to check the consistency in the TL-liquid relations.

A. Tomonaga-Luttinger-liquid parameter

The calculated results for the TL-liquid parameter K_ρ are shown in Fig. 5(a) as a function of J_2/t_2 for various strength of t dimerization where the 8-, 12-, 16-site clusters are used although the cluster-size dependence of K_ρ is small.

A limiting case of $J_2/t_2 \rightarrow 0$ may be considered first. The ground state can be obtained by using the first-order degenerate perturbation theory around $J_1 = J_2 = 0$, where the wave function is the same as that in the $U/t \rightarrow \infty$ dimerized Hubbard model, i.e., a product of the state of spinless fermions describing the charge degrees of freedom localized at each dimer and the state describing the spin system. The $2k_F$ -SDW correlation is dominant here: there is no chance for superconductivity. Note that even if the additional three-site terms are present, which are obtained through the Schrieffer-Wolff transformation to derive the dimerized t - J model from the dimerized Hubbard model, they do not bring any change in the wave function in the first-order perturbation. Consequently, the dimerized t - J model in the $J_2/t_2 \rightarrow 0$ limit for any \tilde{t}_d values gives us the value of $K_\rho = 1/2$. We note, however, that at $J_2/t_2 = 0$ with a finite t dimerization, the charge gap is positive $\Delta_c/t_2 > 0$ and the system is a Mott insulator.

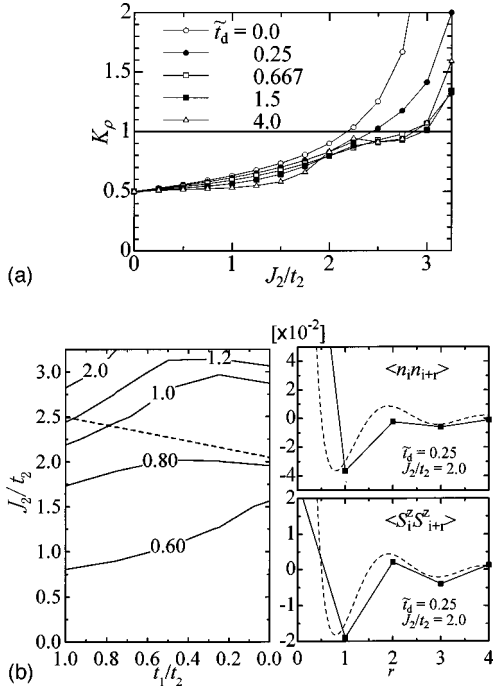


FIG. 5. (a) TL-liquid parameter K_ρ as a function of J_2/t_2 . (b) Contour map for K_ρ on the $(t_1/t_2, J_2/t_2)$ plane where the dotted line is the boundary between the finite spin-gap and gapless regions (left panel) and distance r dependence of the charge and spin correlation functions where dotted lines are from Eqs. (11) and (12) (right panel).

With increasing J_2/t_2 , at any \tilde{t}_d , K_ρ increases, and in the intermediate strength of J_2/t_2 (and for a rather small \tilde{t}_d), there appears the region with $K_\rho > 1$ where the superconducting correlation is the most dominant. In the g -ology, this means the region of $g_2 < 0$ is effectively realized due to the attraction interaction caused by the J dimerization.

In Fig. 5(b), we show the contour map for K_ρ on the parameter space $(t_1/t_2, J_2/t_2)$ where the contour lines are drawn by using a spline interpolation. We find that, for a fixed J_2/t_2 , K_ρ decreases as t dimerization increases. But as shown above the spin gap are enhanced by the increase of t dimerization, so that the phase with both $\Delta_s > 0$ and $K_\rho > 1$ is realized in a reasonably wide range of the parameter values. We thus confirm that the singlet superconducting phase indeed exists. We also find that the calculated spin and charge correlation functions fit very well with Eqs. (11) and (12) as seen in Fig. 5(b).

B. Drude weight and flux quantization

The calculated results for the Drude weight defined in Eq. (17) are shown in Fig. 6. We find that, as t dimerization increases, the dependence of D on J_2/t_2 becomes stronger, and in the strong t -dimerization limit, D approaches the value 0 around the phase-separation point. The numerical technique used here is to thread the cluster ring with a flux Φ and study the functional form of the ground-state energy with respect to the threaded flux, $E_0(\Phi)$. In general, $E_0(\Phi)$ consists of a series of parabola, corresponding to the curves of the individual many-body states $E_n(\Phi)$. This envelope exhibits a periodicity of 1 in units of the flux quantum Φ_0

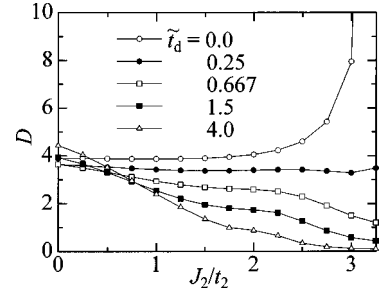


FIG. 6. Drude weight D as a function of J_2/t_2 .

$=hc/e$. The function $E_0(\Phi)$ (or the Drude weight and superfluid density) also yields information on the phenomenon of anomalous flux quantization; one may simply include the effect of a constant vector potential along the ring by the gauge transformation

$$\hat{c}_{j\sigma} \rightarrow \hat{c}_{j\sigma} e^{ij\phi}, \quad \hat{c}_{j\sigma}^\dagger \rightarrow \hat{c}_{j\sigma}^\dagger e^{-ij\phi} \quad (18)$$

where

$$\phi = \frac{2\pi}{N_s} \frac{\Phi}{\Phi_0}. \quad (19)$$

The existence of minima at intervals of half a flux quantum, which is the anomalous flux quantization, clearly indicates the existence of pairing in the thermodynamic limit if the minimum at $\phi = \pi$ decreases with increasing the system size. In Fig. 7, we show the calculated results for the flux quantization for various parameter values in the 8-, 12-, and 16-site clusters to see the system-size dependence. We find that for $\tilde{t}_d = 0$ (i.e., the uniform t - J model), the anomalous flux quantization is not observed, but it occurs in the region where the binding energy is negative. At any strength of t dimerization we find that the anomalous flux quantization occurs for appropriate strength of J dimerization.

In order to check the consistency of the TL-liquid relations, we compare the charge velocity obtained by two independent methods: one is from Eq. (15), and the other is from the relation

$$v_c = \sqrt{\frac{D}{\pi\kappa}} \quad (20)$$

derived from Eqs. (14) and (17). The result is shown in Fig. 8, where we find that the reasonable consistency is indeed achieved.

IV. PHASE DIAGRAM

By summarizing the results for a number of quantities obtained in the previous sections, we now draw the phase diagram of the 1D dimerized t - J model at quarter-filling on the parameter space of t and J dimerizations. The result is shown in Fig. 9.

When the value of J_2/t_2 (or the strength of J dimerization) is very large, the system is phase-separated, which occurs around $J_2/t_2 \approx 3$ when $t_d \rightarrow 0$ and extends to the large \tilde{t}_d region. The critical strength of J_2/t_2 is almost independent of \tilde{t}_d . The phase separated region is determined by the condition $\kappa < 0$. When t dimerization is dominant over J dimer-

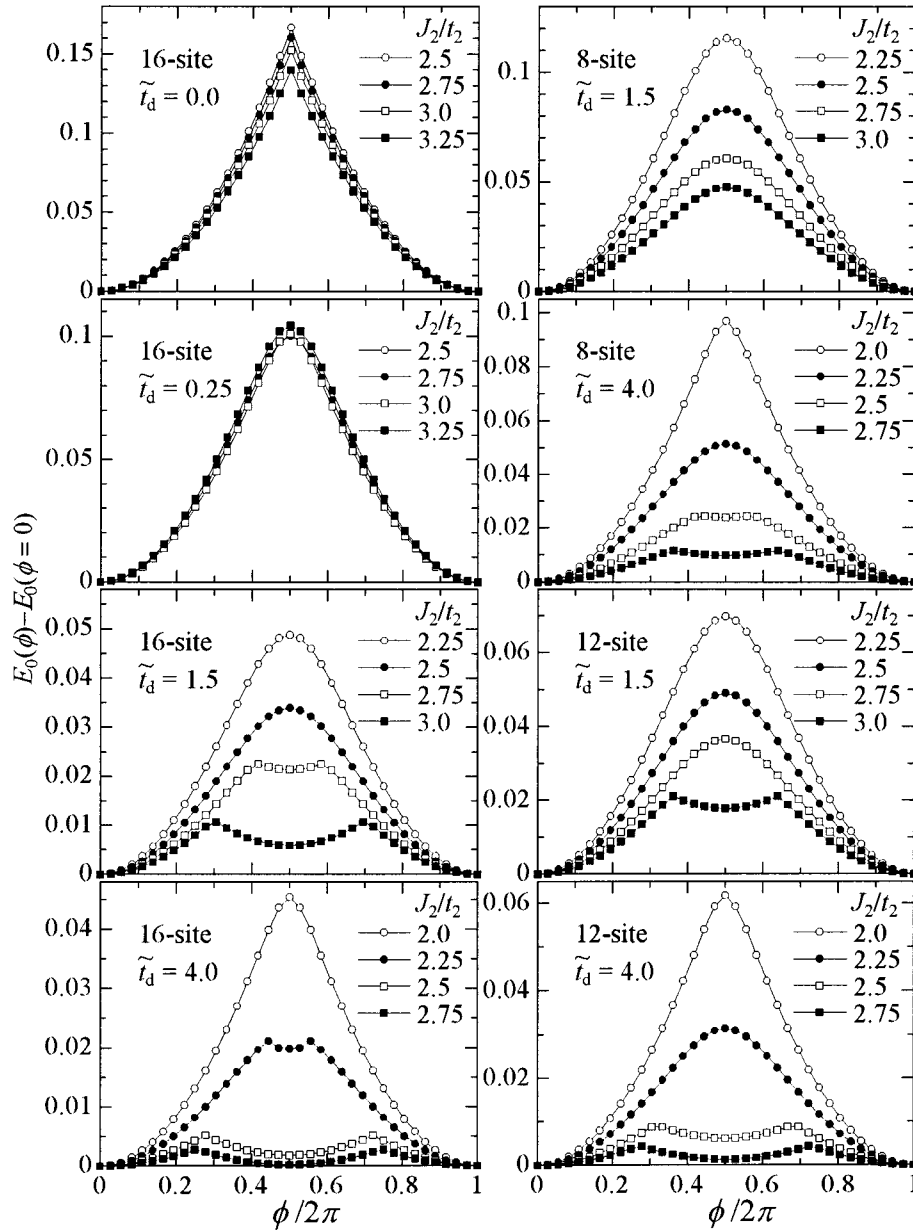


FIG. 7. Energy difference $E_0(\phi) - E_0(0)$ as a function of an external flux ϕ for various parameter values. The results for the 8-, 12-, and 16-site clusters are shown to confirm the minimum structure at $\phi = \pi$ develops with increasing system size.

ization, we find that the system becomes a Mott insulator, where the phase boundary is determined from the calculated values of the charge gap. On the other hand, when J dimerization is dominant over t dimerization, the system becomes metallic or superconducting. We note that there always appears the region of the TL-liquid phase between the region of the Mott insulating phase and the region of the spin-gap liquid phase. The phase boundary between the TL-liquid and spin-gap-liquid regions is determined from the calculated values of the spin gap although whether the spin-gap region exists in the homogeneous t - J model at quarter filling is not clear from our exact-diagonalization data.¹³ In the limit of strong t dimerization (i.e., $\tilde{t}_d \rightarrow \infty$), the model represents an assembly of isolated dimers and the system is an insulator in the entire region of J_2/t_2 unless the phase separation occurs.

We have thus established the overall phase diagram of the dimerized t - J model at quarter-filling, of which not even

very rough features are known so far. We should, however, note that the phase boundary are determined from small-cluster data for a very limited number of system sizes, i.e., 8, 12, and 16 sites with a simple extrapolation to the infinite system, which should therefore be seen with some caution although we believe that the result is valid at least qualitatively. A more sophisticated method such as the renormalization-group analysis developed successfully in Ref. 13 for obtaining the phase diagram of the 1D homogeneous t - J model would be useful to provide more convincing arguments on the phase diagram of the present dimerized t - J model. We hope that our work presented in this paper will promote such a study in the near future.

As for a possible correspondence of the phase diagram with experiment, we may refer to a Bechgaard salt $(\text{TMTTF})_2\text{X}$ where the dimerization strength of $\tilde{t}_d \approx 0.1$ is reported and the Mott-insulator to metal transition induced

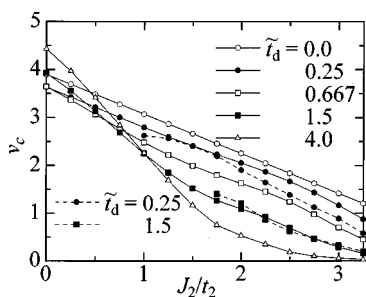


FIG. 8. Charge velocity v_c as a function of J_2/t_2 . The solid lines with symbols represent the value estimated from Eq. (15) and the dashed lines with symbols represent the value estimated from Eq. (20).

by pressure has been observed.^{23,24} We could argue that our phase diagram includes this phase transition around $\tilde{t}_d \approx 0.1$ and $J_2/t_2 \approx 0.3$, provided that the organic system can be described by the dimerized t - J model with a reasonable range of the parameter values J/t .

We have also examined the phase diagram of the 2D dimerized t - J model at quarter-filling²⁵ and found that the phase boundary between the Mott insulating phase and the liquid phase has quite similar parameter dependence. This suggests that, irrespective of the spatial dimensions, the same mechanism discussed in Sec. II A operates in the present insulator-metal (or insulator-superconductor) transition in the quarter-filled dimerized t - J model. The main difference between the 1D and 2D systems is that in 1D the transition from the Mott insulator is to the TL-liquid region whereas in 2D it is to the singlet superconducting region.

V. CONCLUSION

We have studied the ground state of the one-dimensional dimerized t - J model at quarter-filling by using an exact-diagonalization technique on small clusters to calculate the ground-state properties such as the charge gap, spin gap, binding energy, Tomonaga-Luttinger-liquid parameter, Drude weight, anomalous flux quantization, etc. Thereby we have shown that the two types of dimerization, i.e., a dimerization of hopping integral (called t dimerization) and a dimerization of exchange interaction (called J dimerization), plays an essential and mutually competing role in controlling the electronic ground state of the system; the t dimerization has the effect leading to the repulsive interaction among electrons in a dimer and the J dimerization has the effect

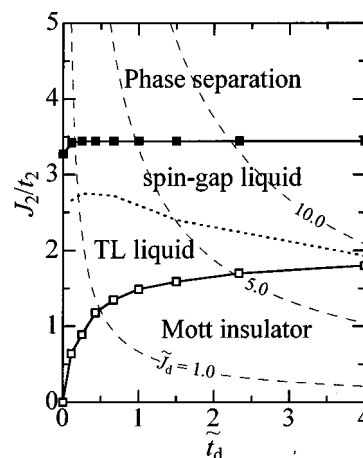


FIG. 9. Phase diagram of the 1D dimerized t - J model at quarter filling on the parameter space of t and J dimerizations. Dotted line separates the spin-gap-liquid region from the TL-liquid region. The contour of constant \bar{J}_d is also shown by dashed lines.

promoting the spin-singlet formation in a dimer. The resulting noticeable features we have obtained are the following: (i) The competition between t and J dimerizations induce the metal-insulator transition. (ii) There always appears the region of the TL-liquid phase between the region of Mott insulating phase and the region of the spin-gap-liquid phase. (iii) The spin gap and singlet binding energy are enhanced by the increase of dimerizations. We have summarized the calculated results as the phase diagram in the parameter space of dimerizations.

Finally we would emphasize that the correlated electron systems at (and around) quarter-filling indeed exhibit interesting properties as we have seen and further studies should be pursued in other quarter-filled systems from both theoretical and experimental sides.

ACKNOWLEDGMENTS

This work was supported in part by a Grant-in-Aid for Scientific Research from the Ministry of Education, Science, and Culture of Japan. The financial support of S. N. by Sasakawa Scientific Research Grant from the Japan Science Society, and of Y. O. by Iketani Science and Technology Foundation, are gratefully acknowledged. Computations were carried out in Computer Centers of the Institute for Solid State Physics, University of Tokyo and the Institute for Molecular Science, Okazaki National Research Organization.

¹For a review, see D. Jérôme, in *Organic Conductors*, edited by J. P. Farges (Dekker, New York, 1994).

²H. Seo and H. Fukuyama, *J. Phys. Soc. Jpn.* **66**, 1249 (1997).

³K. Penc and F. Mila, *Phys. Rev. B* **50**, 11 429 (1994).

⁴T. Ohama, H. Yasuoka, M. Isobe, and Y. Ueda, *Phys. Rev. B* (to be published).

⁵H. Smolinski, C. Gros, W. Weber, U. Peuchert, G. Roth, M. Weiden, and C. Geibel, *Phys. Rev. Lett.* **80**, 5164 (1998).

⁶P. Horsch and F. Mack, *Eur. Phys. J. B* **5**, 367 (1998).

⁷K. Takenaka, Y. Imanaka, K. Tamasaku, T. Ito, and S. Uchida, *Phys. Rev. B* **46**, 5833 (1992).

⁸B. Grévin, Y. Berthier, G. Collin, and P. Mendels, *Phys. Rev. Lett.* **80**, 2405 (1998).

⁹M. Imada, *Phys. Rev. B* **48**, 550 (1993).

¹⁰M. Ogata, M. U. Luchini, S. Sorella, and F. F. Assaad, *Phys. Rev. Lett.* **66**, 2388 (1991).

¹¹H. Yokoyama and M. Ogata, *Phys. Rev. Lett.* **67**, 3610 (1991).

¹²H. Shiba and M. Ogata, *Prog. Theor. Phys. Suppl.* **108**, 265 (1992).

¹³M. Nakamura, K. Nomura, and A. Kitazawa, *Phys. Rev. Lett.* **79**, 3214 (1997); M. Nakamura, *J. Phys. Soc. Jpn.* **67**, 717 (1998).

¹⁴E. Dagotto, *Rev. Mod. Phys.* **66**, 763 (1994).

- ¹⁵P. Nozières and S. Schmitt-Rink, *J. Low Temp. Phys.* **59**, 195 (1985).
- ¹⁶H. J. Schulz, *Phys. Rev. Lett.* **64**, 2831 (1990); *Int. J. Mod. Phys. B* **5**, 57 (1991).
- ¹⁷N. Kawakami and S. K. Yang, *Phys. Lett. A* **148**, 359 (1990).
- ¹⁸H. Frahm and V. E. Korepin, *Phys. Rev. B* **42**, 10 553 (1990).
- ¹⁹W. Kohn, *Phys. Rev.* **133**, A171 (1964).
- ²⁰B. S. Shastry and B. Sutherland, *Phys. Rev. Lett.* **65**, 243 (1990).
- ²¹A. Ferreti, I. O. Kulik, and A. Lami, *Phys. Rev. B* **45**, 5486 (1992).
- ²²J. Voit, *Rep. Prog. Phys.* **58**, 977 (1995).
- ²³S. S. P. Parkin, C. Coulon, and D. Jérôme, *J. Phys. C* **16**, L209 (1983).
- ²⁴K. Murata, H. Anzai, T. Ukachi, and T. Ishiguro, *J. Phys. Soc. Jpn.* **53**, 491 (1984).
- ²⁵S. Nishimoto and Y. Ohta, *J. Phys. Soc. Jpn.* **67**, 2598 (1998).